

Energy Harvesting Communications Under Explicit and Implicit Temperature Constraints

Abdulrahman Baknina, *Student Member, IEEE*, Omur Ozel, *Member, IEEE*, and Sennur Ulukus[✉], *Fellow, IEEE*

Abstract—With a motivation to understand the effects of temperature sensitivity on wireless data transmission performance, we consider an energy harvesting communication system, where the temperature dynamics are governed by the transmission power policy. Different from the previous work, we consider a discrete time system where transmission power is kept constant in each slot. We consider two models that capture different effects of temperature. In the first model, the temperature is constrained to be below a critical temperature at all time instants; we coin this the *explicit temperature constrained model*. We investigate throughput optimal power allocation for multiple energy arrivals under general, as well as temperature and energy limited regimes. We show that the optimal power allocation for the temperature limited case is monotone decreasing. In the second model, we consider the effect of the temperature on the channel quality via its influence on additive noise power; we coin this the *implicit temperature constrained model*. In this model, the change in the variance of the additive noise due to previous transmissions is non-negligible. In particular, transmitted signals contribute as interference for all subsequent slots and thus affect the signal to interference plus noise ratio (SINR). In this case, we investigate throughput optimal power allocation under general, as well as low and high SINR regimes. We show in the low SINR regime that the optimal allocation dictates the transmitter to save its harvested energy till the last slot. In the high SINR regime, we show that the optimal power sequence is monotone increasing. Finally, we consider the case in which implicit and explicit temperature constraints are simultaneously active and we show under certain conditions that the optimal power sequence is monotone decreasing.

Index Terms—Energy harvesting communications, temperature constraints, power control, throughput maximization.

I. INTRODUCTION

DEUE to physical principles that govern the heating effect of electromagnetic radiation, wireless sensors are by nature prone to temperature increase caused by sensor operation.

Manuscript received September 10, 2017; revised February 6, 2018 and May 30, 2018; accepted July 19, 2018. Date of publication August 8, 2018; date of current version October 9, 2018. This work was supported by NSF Grants CNS 13-14733, CCF 14-22111, and CNS 15-26608. This paper was presented in part at the IEEE Global Communications Conference, Singapore, December 2017. The editor coordinating the review of this paper and approving it for publication was J. Zhang. (Corresponding author: Sennur Ulukus.)

A. Baknina and S. Ulukus are with the Department of Electrical and Computer Engineering, University of Maryland at College Park, College Park, MD 20742 USA (e-mail: abaknina@umd.edu; ulukus@umd.edu).

O. Ozel is with the Department of Electrical and Computer Engineering, Carnegie Mellon University, Pittsburgh, PA 15213 USA (e-mail: omurozel@ieee.org).

Color versions of one or more of the figures in this paper are available online at <http://ieeexplore.ieee.org>.

Digital Object Identifier 10.1109/TWC.2018.2861874

The temperature of the surrounding environment, transmit power for data transmission, and circuit power associated with processing all play roles in the time dynamics for temperature in wireless sensors. In this regard, temperature increase caused by sensor operation may be a limiting factor in many applications. While this issue is tackled in the design of the hardware with sufficient heat sinks for the least amount of heat dissipation, in many temperature sensitive wireless sensor applications the hazardous effect of heating has to be carefully managed. This problem arises in various types of biomedical wireless sensor networks [1]–[3] where depending on the type of tissue and material properties of the sensor node, data transmission has to be scheduled according to temperature sensitivity [4]. More generally, temperature increase in a sensor is a threat for the proper operation of the hardware [5], [6] and therefore, the electric power that feeds the communication circuitry has to be carefully scheduled to avoid heat related damage.

With a motivation to understand the effects of temperature sensitivity on wireless data transmission performance, we build on our recent works [7], [8] and consider data transmission with energy harvesting sensors under temperature constraints. In the current work, our particular focus is to contrast two different effects of temperature on the optimal power allocation in a single-user energy harvesting communication system. These effects show themselves as explicit and implicit temperature constraints on the power allocation. We determine throughput optimal offline power scheduling policies under energy harvesting constraints along with explicit and implicit temperature constraints. Transmission scheduling problems under energy harvesting constraints only have been studied in various works in the literature, see [9]–[35]. Previous works considered single-user channel [9]–[12], broadcast channel [13], multiple access channel [14], [15], interference channel [16], two-hop channel [17]–[19], two-way channel [20], [21], and diamond channel [22]. The effect of imperfect transmitter circuitry is considered in [23]–[29]. Receiver side energy harvesting communication systems is considered in [30]–[35].

In contrast to our earlier works [7], [8], in this paper we consider the scheduling problem under energy harvesting and temperature constraints in discrete time. Our interest in discrete time solution stems from the fact that circuits typically run on digital clocks and decisions on the transmission strategy are taken on discrete time intervals. In the first model we consider here, which we coin as the *explicit temperature constrained model*, we consider an explicit peak temperature

constraint as in [7] and obtain a discrete time version of the problem considered in [7]. In this temperature constrained problem, increasing the transmission power increases the throughput and the temperature. Due to the fixed temperature budget, higher temperature levels mean smaller admissible transmission power levels for future slots. When the temperature constraint is not binding, the problem reduces to the single-user energy harvesting channel studied in [9], where the optimal power sequence is monotone increasing. When the energy constraint is not binding, we show that the optimal power sequence is monotone decreasing, and the resulting temperature is monotone increasing.

In the second model we consider here, which we coin as the *implicit temperature constrained model*, the temperature is not explicitly constrained, however, the temperature affects the additive noise power and hence the channel quality. This problem arises when the dynamic range of the temperature is large and affects the noise added at the receiver circuitry in the spirit of [36]. Our current focus is to investigate this problem in a scheduling-theoretic setting. In this case, the transmit powers used in earlier time slots affect the thermal noise in the form of intersymbol interference, and hence, the channel becomes a *use dependent* or *action dependent* channel, see [37]–[39]. Our work represents, to the best of our knowledge, the first instance of this implicit temperature constrained problem in the context of energy harvesting communications.

In the implicit temperature constrained model, transmissions in the previous slots interfere with the current transmission due to temperature dependent noise and the causality of the temperature filter. This filter is the discrete time version of the continuous time first order filter that defines the temperature dynamics. For the general signal to interference plus noise ratio (SINR), we observe that the problem is non-convex and is a signomial problem for which we obtain a local optimal solution using the single condensation method in [40]. We then propose a heuristic algorithm which improves upon the local optimal solution and may achieve the global optimal solution. Then, we consider the extreme settings of low and high SINR regimes. We show that in the low SINR regime, saving energy till the last slot and transmitting only in the last slot is optimal. For the high SINR regime, we observe that the problem is a *geometric program* and we explore specific structural results in this setting. Expanding upon the equivalence of this problem to its convex counterpart via a one-to-one transformation, we show that the KKT conditions in the original problem have a unique solution. Then, we obtain an algorithm to solve the KKT conditions in the original problem. We show convergence of this algorithm to the unique solution of the KKT conditions. We then show that for this unique solution, the power sequence is monotone increasing; hence, proving the monotone increasing property of the optimal power sequence.

Finally, we consider the case when implicit and explicit temperature constraints are simultaneously active. In general, we observe that the problem is non-convex and the same signomial programming approach as in the implicit temperature constrained case is applicable. In the high SINR regime, the problem is a geometric program and we show in the

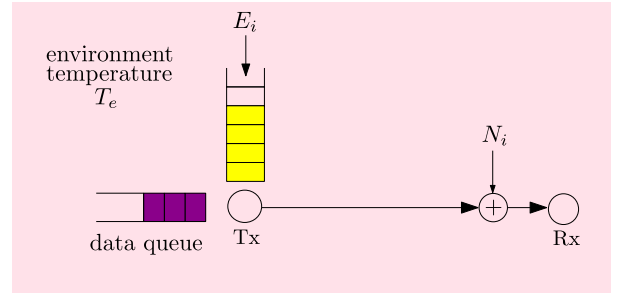


Fig. 1. System model: the system heats up due to data transmission.

temperature limited case that the optimal power sequence is monotone decreasing under certain conditions. We illustrate our findings in various numerical results.

II. SYSTEM MODEL

We consider an energy harvesting communication system in which the transmitter harvests energy \tilde{E}_i in the i th slot, see Fig. 1. We consider the temperature model considered in [7] and [8]. In this model, the temperature, $T(t)$, evolves according to the following differential equation,

$$\frac{dT(t)}{dt} = ap(t) - b(T(t) - T_e) \quad (1)$$

where T_e is the environment temperature, $T(t)$ is the temperature at time t , $p(t)$ is the power, and a, b are non-negative constants. With the initial temperature $T(0) = T_e$, the solution of (1) is:

$$T(t) = e^{-bt} \int_0^t e^{b\tau} ap(\tau) d\tau + T_e \quad (2)$$

In what follows we assume that the duration of each slot is equal to Δ , which can take any positive value. Let us define $T_i \triangleq T(i\Delta)$ as the temperature level by the end of the i th slot, $P_i \triangleq P(i\Delta)$ as the power level used in the i th slot. Using (2), T_i can be expressed as:

$$T_i = e^{-bi\Delta} \int_0^{i\Delta} e^{b\tau} ap(\tau) d\tau + T_e \quad (3)$$

$$= e^{-b\Delta} e^{-b(i-1)\Delta} \int_0^{(i-1)\Delta} e^{b\tau} ap(\tau) d\tau + e^{-bi\Delta} \int_{(i-1)\Delta}^{i\Delta} e^{b\tau} aP_i d\tau + T_e \quad (4)$$

$$= e^{-b\Delta} (T_{i-1} - T_e) + \frac{aP_i}{b} [1 - e^{-b\Delta}] + T_e \quad (5)$$

$$= \alpha T_{i-1} + \beta P_i + \gamma \quad (6)$$

where $\alpha = e^{-b\Delta}$, $\beta = \frac{a}{b} [1 - \alpha]$ and $\gamma = T_e [1 - \alpha]$.

The effect of Δ in (6) appears through the constants α, β, γ . As the slot duration increases, the values of β, γ increase while the value of α decreases; as the slot duration increases, the temperature at the end of the slot becomes more dependent on the power transmitted within this slot and less dependent on the initial temperature at the beginning of the slot.

We now eliminate the previous temperature readings in T_i making the temperature a function of the powers only. We can do this by recursively substituting T_{i-1} in T_i in (6) to have

$$T_k = \beta \sum_{i=1}^k \alpha^{k-i} P_i + T_e \quad (7)$$

This formula shows that the temperature at the end of each slot depends on the power transmitted in this slot and all previous slots through an exponentially decaying *temperature filter*. We note that this is the same formula that was developed in [36] in which the slot duration was assumed to be unity; here we assume a general slot duration which is equal to Δ . In what follows, we denote the vector of elements by the bold letter without a subscript, i.e., for example, the vector of powers is defined as $\mathbf{P} \triangleq [P_1, \dots, P_D]$.

III. EXPLICIT PEAK TEMPERATURE CONSTRAINT

We now consider the model in which we have an energy harvesting transmitter with a peak temperature constraint. The noise variance is the same throughout the communication session and is set to σ^2 . We consider a slotted system with a constant power per slot. There are D slots. It follows from (4) (and also [7, eq. (47)]), that the temperature is monotone within the slot duration. Hence, for the peak temperature constrained case, it suffices to constrain the temperature only at the end of each slot; we begin the communication with the system having temperature T_e . In this case, the problem can be written as

$$\begin{aligned} \max_{\mathbf{P} \geq 0} \quad & \sum_{i=1}^D \frac{\Delta}{2} \log \left(1 + \frac{P_i}{\sigma^2} \right) \\ \text{s.t.} \quad & T_k \leq T_c \\ & \sum_{i=1}^k \Delta P_i \leq \sum_{i=1}^k \tilde{E}_i, \quad \forall k \end{aligned} \quad (8)$$

where Δ in the objective function and the energy constraint is to account for the slot duration. In what follows, without loss of generality, we drop Δ since it is just a constant multiplied in the objective function and by defining $E_i = \frac{\tilde{E}_i}{\Delta}$.

We rewrite problem (8) making use of (7) as

$$\begin{aligned} \max_{\mathbf{P} \geq 0} \quad & \sum_{i=1}^D \frac{1}{2} \log \left(1 + \frac{P_i}{\sigma^2} \right) \\ \text{s.t.} \quad & \sum_{i=1}^k \alpha^{k-i} P_i \leq \frac{T_c - T_e}{\beta} \\ & \sum_{i=1}^k P_i \leq \sum_{i=1}^k E_i, \quad \forall k \end{aligned} \quad (9)$$

In the last slot, either the temperature or the energy constraint has to be satisfied with equality. Otherwise, we can increase one of the powers until one of the constraints is met with equality and this strictly increases the objective function.

This problem is a convex problem, which can be solved optimally using the KKT conditions. The Lagrangian function

for (9) is:

$$\begin{aligned} \mathcal{L} = - \sum_{i=1}^D \log \left(1 + \frac{P_i}{\sigma^2} \right) + \sum_{k=1}^D \lambda_k \left(\sum_{i=1}^k \alpha^{k-i} P_i - \frac{T_c - T_e}{\beta} \right) \\ + \sum_{k=1}^D \mu_k \left(\sum_{i=1}^k P_i - \sum_{i=1}^k E_i \right) \end{aligned} \quad (10)$$

where λ_k and μ_k represent the Lagrange multipliers corresponding to the first set and the second set of constraints in (9), respectively. Differentiating with respect to P_i and equating to zero we get,

$$P_i = \left(\frac{1}{\alpha^{-i} \sum_{k=i}^D \lambda_k \alpha^k + \sum_{k=i}^D \mu_k} - \sigma^2 \right)^+ \quad (11)$$

where $(x)^+ = \max\{x, 0\}$. Additionally, the corresponding complementary slackness conditions are

$$\lambda_k \left(\sum_{i=1}^k \alpha^{k-i} P_i - \frac{T_c - T_e}{\beta} \right) = 0 \quad (12)$$

$$\mu_k \left(\sum_{i=1}^k P_i - \sum_{i=1}^k E_i \right) = 0 \quad (13)$$

In the optimal solution, if neither constraint was tight in slot $i < D$, then the power in slot $i+1$ is strictly less than the power in slot i . This follows from complementary slackness in (12)-(13) since if at slot i , if both constraints were not tight then we have $\lambda_i = \mu_i = 0$ which, using (11), implies that $P_i > P_{i+1}$.

In the following two subsections, we consider special cases of (9) which we call *energy limited case* and *temperature limited case*. In the energy limited case, the temperature budget is sufficiently large so that the problem reduces to that limited by the energy constraints only. In the temperature limited case, energy budget is sufficiently large so that the problem reduces to that limited by temperature constraints only.

A. Energy Limited Case

In this subsection, we study a sufficient condition under which the system becomes energy limited, i.e., when the temperature budget is sufficiently large so that the temperature constraints are not binding. For all slots j in which the following is satisfied

$$\sum_{i=1}^j E_i \leq \frac{T_c - T_e}{\beta} \quad (14)$$

the temperature constraint cannot be tight. Intuitively, in this case, the incoming energy is so small that it can never overheat the system. Therefore, the binding constraint here is the availability of energy. In particular, when (14) is satisfied for $j = D$, then the temperature constraint can be completely removed from the system. To prove this, we assume for the sake of contradiction that we have at slot j , $\sum_{i=1}^j E_i \leq \frac{T_c - T_e}{\beta}$ while the temperature constraint is tight, which implies:

$$\frac{T_c - T_e}{\beta} = \sum_{i=1}^j \alpha^{j-i} P_i < \sum_{i=1}^j P_i \leq \sum_{i=1}^j E_i \quad (15)$$

which contradicts the assumption $\sum_{i=1}^j E_i \leq \frac{T_c - T_e}{\beta}$. The strict inequality follows since $\alpha < 1$. The structure of the optimal solution for this case is studied in [9].

B. Temperature Limited Case

In this subsection, we first study a sufficient condition for problem (9) to be temperature limited, i.e., when the energy budget is sufficiently large so that the energy constraints are not binding. The energy constraint is never tight if the following condition is satisfied:

$$\frac{T_c - T_e}{\beta} < \frac{\sum_{i=1}^k E_i}{k}, \quad \forall k \in \{1, \dots, D\} \quad (16)$$

Intuitively, the incoming energy is so large that there will never be a shortage of energy. Therefore, the binding constraint here is overheating the system. For the temperature limited case, an upper bound on the transmission powers is equal to $\frac{T_c - T_e}{\beta}$. This follows because for any slot k we have $\sum_{i=1}^{k-1} \alpha^{k-i} P_i + P_k \leq \frac{T_c - T_e}{\beta}$, thus P_k can be at most equal to $\frac{T_c - T_e}{\beta}$. Hence, (16) is sufficient to satisfy $\sum_{i=1}^k P_i < \sum_{i=1}^k E_i$.

In what follows, we study the structure of the optimal policy for the temperature limited case. In the last slot, the temperature constraint is satisfied with equality. The optimal powers are monotonically decreasing in time. The proof follows by contradiction. Assume for some index j that we have $P_j^* < P_{j+1}^*$. We now form another policy, denoted as $\{\bar{P}_i\}$, which has $\bar{P}_i = P_i^*$ for all slots $i \neq j, j+1$, while we change the powers of slots $j, j+1$ to be $\bar{P}_j = P_j^* + \delta$ and $\bar{P}_{j+1} = P_{j+1}^* - \delta$ for small enough $\delta > 0$. This δ always exists as $P_j^* < P_{j+1}^*$ implies that $\sum_{k=1}^j \alpha^{j-k} P_k^* < \frac{T_c - T_e}{\beta}$. Since the objective function is strictly concave, this new policy yields a strictly higher objective function, which contradicts the optimality of $P_j^* < P_{j+1}^*$. Now it remains to check that with this new policy, the temperature constraint is still feasible for any slot $k \geq j+1$ which follows from:

$$\begin{aligned} & \sum_{i=1, \neq j, j+1}^k \alpha^{k-i} \bar{P}_i + \alpha^{k-j} \bar{P}_j + \alpha^{k-j-1} \bar{P}_{j+1} \\ &= \sum_{i=1, \neq j, j+1}^k \alpha^{k-i} P_i^* + \alpha^{k-j} \bar{P}_j + \alpha^{k-j-1} \bar{P}_{j+1} \end{aligned} \quad (17)$$

$$< \sum_{i=1, \neq j, j+1}^k \alpha^{k-i} P_i^* + \alpha^{k-j} P_j^* + \alpha^{k-j-1} P_{j+1}^* \quad (18)$$

$$= \sum_{i=1}^k \alpha^{k-i} P_i^* \quad (19)$$

$$< \frac{T_c - T_e}{\beta} \quad (20)$$

Since this is valid for any $k \geq j+1$, we can take in particular $k = D$. Now we can increase any of the powers to satisfy the last inequality by equality which strictly improves the objective function. Hence, this violates the optimality of any policy which has $P_i^* < P_{i+1}^*$ for any $i \in \{1, \dots, D\}$.

Moreover, the optimal temperature levels are non-decreasing in time. To prove this, using (7), it suffices to show that:

$$\sum_{i=1}^k \alpha^{k-i} P_i^* \leq \sum_{i=1}^{k+1} \alpha^{k+1-i} P_i^*, \quad \forall k = \{1, \dots, D-1\} \quad (21)$$

We rewrite (21) as follows,

$$(1-\alpha) \sum_{i=1}^k \alpha^{k-i} P_i^* \leq P_{k+1}^*, \quad \forall k = \{1, \dots, D-1\} \quad (22)$$

Since, we know that the last slot has to be satisfied with equality then we know $\sum_{i=1}^D \alpha^{D-i} P_i^* = \frac{T_c - T_e}{\beta}$. Hence, for the constraint at $k = D-1$ we have:

$$\sum_{i=1}^{D-1} \alpha^{D-1-i} P_i^* \leq \frac{T_c - T_e}{\beta} = \sum_{i=1}^D \alpha^{D-i} P_i^* \quad (23)$$

which can be written as follows

$$(1-\alpha) \sum_{i=1}^{D-1} \alpha^{D-1-i} P_i^* \leq P_D^* \quad (24)$$

which proves (22) for $k = D-1$. Now assume for the sake of contradiction that (22) is false for $k = D-2$, i.e.:

$$P_{D-1}^* < (1-\alpha) \sum_{i=1}^{D-2} \alpha^{D-2-i} P_i^* \quad (25)$$

Substituting this in (24), we get:

$$P_{D-1}^* = \alpha P_{D-1}^* + (1-\alpha) P_{D-1}^* \quad (26)$$

$$< \alpha(1-\alpha) \sum_{i=1}^{D-2} \alpha^{D-2-i} P_i^* + (1-\alpha) P_{D-1}^* \quad (27)$$

$$= (1-\alpha) \sum_{i=1}^{D-1} \alpha^{D-1-i} P_i^* \leq P_D^* \quad (28)$$

But since we know that in the optimal policy the power sequence is monotone decreasing, this is a contradiction and (22) holds for $k = D-2$. The same argument follows for any $k < D-2$.

In the optimal solution, if the constraint is satisfied with equality for two consecutive slots then the power in the second slot must be equal to $(1-\alpha) \frac{T_c - T_e}{\beta}$. To obtain this, the two consecutive constraints which are satisfied with equality are solved simultaneously for the power in the second slot. In addition, when the temperature hits the critical temperature for the first time, the transmission power in that slot will be *strictly higher* than $(1-\alpha) \frac{T_c - T_e}{\beta}$. To show this we denote the time slot at which the temperature hits T_c for the first time as i^* . Hence, we have:

$$\sum_{i=1}^{i^*-1} \alpha^{i^*-1-i} P_i < \frac{T_c - T_e}{\beta}, \quad \sum_{i=1}^{i^*} \alpha^{i^*-i} P_i = \frac{T_c - T_e}{\beta} \quad (29)$$

Using both equations in (29) simultaneously we have:

$$(1-\alpha) \frac{T_c - T_e}{\beta} < P_{i^*} \quad (30)$$

which is the power of the slot at which temperature hits the critical temperature for the first time.

Hence, when the temperature hits the critical temperature, the optimal transmission power in all the subsequent slots becomes constant and equal to $(1 - \alpha) \frac{T_c - T_e}{\beta}$. This follows since the temperature is increasing, thus whenever the constraint becomes tight, it remains tight for all subsequent slots. We now conclude that the transmission power at all slots are bounded as follows

$$(1 - \alpha) \frac{T_c - T_e}{\beta} \leq P_i \leq \frac{T_c - T_e}{\beta}, \quad \forall i = \{1, \dots, D\} \quad (31)$$

The lower bound follows from the discussion above while the upper bound follows from the feasibility of the constraints.

We now proceed to find the optimal power allocation. Since the problem is convex, a necessary and sufficient condition is to find a solution satisfying the KKTs. The optimal power is given by setting $\mu = 0$ in (11), which gives:

$$P_i = \left(\frac{\alpha^i}{\sum_{k=i}^D \lambda_k \alpha^k} - \sigma^2 \right)^+ \quad (32)$$

It follows from the complementary slackness that if at slot i the temperature constraint is satisfied with strict inequality then $P_{i+1} < P_i$.

IV. IMPLICIT TEMPERATURE CONSTRAINT

We now consider the case when the dynamic range of the temperature increases. In this case, we need to consider the change in the thermal noise of the system due to temperature changes. The thermal noise is linearly proportional to the temperature [41, Ch. 11]. The problem can be written as:

$$\begin{aligned} \max_{\mathbf{P} \geq \mathbf{0}} \quad & \sum_{i=1}^D \frac{1}{2} \log \left(1 + \frac{P_i}{c T_{i-1} + \sigma^2} \right) \\ \text{s.t.} \quad & \sum_{i=1}^k P_i \leq \sum_{i=1}^k E_i, \quad \forall k \end{aligned} \quad (33)$$

where c is the proportionality constant between the thermal noise and the temperature. In this setting, the noise variance in each slot is determined by the value of the temperature at the beginning of the slot. Using (7) in (33), the problem can now be written in terms of only transmission powers as follows:

$$\begin{aligned} \max_{\mathbf{P} \geq \mathbf{0}} \quad & \sum_{i=1}^D \frac{1}{2} \log \left(1 + \frac{P_i}{c \left(\beta \sum_{k=1}^{i-1} \alpha^{i-1-k} P_k + T_e \right) + \sigma^2} \right) \\ \text{s.t.} \quad & \sum_{i=1}^k P_i \leq \sum_{i=1}^k E_i, \quad \forall k \end{aligned} \quad (34)$$

where we define $\text{SINR}_i \triangleq \frac{P_i}{c \beta \sum_{k=1}^{i-1} \alpha^{i-1-k} P_k + c T_e + \sigma^2}$. In what follows, in order to simplify the notation and facilitate simpler expressions, we assume without loss of generality that $c\beta = 1$ and define $\Gamma_j \triangleq \frac{c T_e + \sigma^2}{\alpha^j}$. Therefore, SINR_i inside the log in (34) becomes $\text{SINR}_i = \frac{P_i}{\sum_{k=1}^{i-1} \alpha^{i-1-k} P_k + \Gamma_0}$. We note that assuming $c\beta = 1$ is not binding for the analytical results we develop in the rest of the paper and we stop using this assumption for the numerical results in Section VI.

The problem in this form highlights the effect of previous transmissions on subsequent slots. The transmission power at time i appears as an *interfering term* at slot indices greater than i with an exponentially decaying weight due to the *filtering* in the temperature. Using (7), the maximum temperature the system can reach is equal to $T_{max} \triangleq \beta \sum_{i=1}^D E_i + T_e$. This occurs when the transmitter transmits all its energy arrivals in the last slot. The value of T_{max} is useful in determining the maximum possible temperature for the system. As we show, in the low SINR case in Section IV-A, the optimal power allocation results in system temperature equal to T_{max} .

The problem in (34) is non-convex and determining the global optimal solution is generally a difficult task. Next, we adapt the signomial programming based iterative algorithm in [40] for the energy harvesting case. This algorithm provably converges to a local optimum point. The problem in (34) can be written in the following equivalent signomial minimization problem

$$\begin{aligned} \min_{\mathbf{P} \geq \mathbf{0}} \quad & \prod_{i=1}^D \left(\frac{\sum_{k=1}^{i-1} \alpha^{i-1-k} P_k + \Gamma_0}{\sum_{k=1}^{i-1} \alpha^{i-1-k} P_k + \Gamma_0 + P_i} \right) \\ \text{s.t.} \quad & \sum_{i=1}^k P_i \leq \sum_{i=1}^k E_i, \quad \forall k \end{aligned} \quad (35)$$

The objective function in (35) is a signomial function which is a ratio between two posynomials. Note also that the energy harvesting constraints in (35) are posynomials in P_i .

In each iteration we approximate the objective by a posynomial. We do this by approximating the posynomial in the denominator by a monomial. Appropriate choice of an approximation which satisfies the conditions in [42] guarantees convergence to a local optimal solution. Let us denote the posynomial in the i th denominator evaluated using a power vector \mathbf{P} by $u_i(\mathbf{P})$, i.e., we have

$$u_i(\mathbf{P}) \triangleq \sum_{k=1}^{i+1} v_k^i(\mathbf{P}) = \sum_{k=1}^{i-1} \alpha^{i-1-k} P_k + P_i + \Gamma_0 \quad (36)$$

where for $k = \{1, \dots, i-1\}$ we have $v_k^i(\mathbf{P}) = \alpha^{i-1-k} P_k$, $v_i^i(\mathbf{P}) = P_i$ and $v_{i+1}^i(\mathbf{P}) = \Gamma_0$.

Using the arithmetic-geometric mean inequality, we approximate each posynomial by a monomial as follows:

$$u_i(\mathbf{P}) \geq \left(\prod_{k=1}^{i-1} \left(\frac{\alpha^{i-1-k} P_k}{\theta_k^i} \right)^{\theta_k^i} \right) \left(\frac{P_i}{\theta_i^i} \right)^{\theta_i^i} \left(\frac{\Gamma_0}{\theta_{i+1}^i} \right)^{\theta_{i+1}^i} \quad (37)$$

where $\sum_{k=1}^{i+1} \theta_k^i = 1$ for all $i = \{1, \dots, D\}$.

We now solve the problem in (35) iteratively. First, we initialize the power allocation to any feasible power allocation \mathbf{P}^0 . Then, we approximate the posynomials $u_i(\mathbf{P}^0)$ using the arithmetic-geometric mean inequality shown above. In each iteration j , where the power allocation is \mathbf{P}^j , we choose θ_k^i as a function of the posynomials and the current power allocation as follows:

$$\theta_k^i(\mathbf{P}^j) = \frac{v_k^i(\mathbf{P}^j)}{u_i(\mathbf{P}^j)} \quad (38)$$

which satisfies $\sum_{k=1}^{i+1} \theta_k^i(\mathbf{P}^j) = 1$. This choice of $\theta_k^i(\mathbf{P}^j)$ guarantees that the iterations converge to a KKT point of

Algorithm 1 Single-Condensation Method

- 1: Initialize $P_i = E_i$
- 2: **repeat**
- 3: For $k = \{1, \dots, i-1\}$, calculate $v_k^i(\mathbf{P}) = \alpha^{i-1-k} P_k$
- 4: Set $v_{i+1}^i(\mathbf{P}) = \Gamma_0$ and $v_i^i(\mathbf{P}) = P_i$
- 5: Calculate $u_i(\mathbf{P})$ using (36)
- 6: Calculate $\theta_k^i(\mathbf{P}^j)$ according to (38)
- 7: Approximate $u_i(\mathbf{P})$ using (37)
- 8: Solve problem (35) using the approximate objective function calculated in Step 7
- 9: **until** Convergence to a local optimal solution

the original problem [42]. In particular, for each iteration this is a geometric program and as required by [42], this can be transformed into a convex problem; see also [40]. A pseudo code for this procedure is provided in Algorithm 1. In each iteration, the computation complexity of finding the solution of the convex problem is polynomial in the number of constraints and the number of variables, see [43].

The above iterative approach converges to a local optimal solution. Achieving the global optimal solution is of exponential complexity. Alternatively, to get to the optimal solution, an approach introduced in [44] can be used. This approach solves the following problem iteratively:

$$\begin{aligned} & \min_{\mathbf{P} \geq \mathbf{0}, t} t \\ & \text{s.t. } O(\mathbf{P}) \leq t \\ & \quad t \leq \frac{t_0}{\alpha} \\ & \quad \sum_{i=1}^k P_i \leq \sum_{i=1}^k E_i, \quad \forall k \end{aligned} \quad (39)$$

where $O(\mathbf{P})$ is the objective function of (35) and α is chosen to be a number which is slightly more than 1 and t_0 can be initialized to be the solution of problem (35) and then updated as the optimal solutions resulting from (39).

This completes our treatment of the general problem for the case of implicit temperature constraints. In the following two subsections, we consider the two special cases of low and high SINR, where we are able to provide more structural solutions.

A. Low SINR Case

The low SINR case occurs when the incoming energies are small with respect to the noise variance. In this case, an approximation to the logarithm function in the objective function is the linear function, i.e., $\log(1+x) \approx x$. Hence, the objective function of (34) can be written as follows, c.f. [45, eq. (14)]:

$$\sum_{i=1}^D \frac{P_i}{\sum_{k=1}^{i-1} \alpha^{i-1-k} P_k + \Gamma_0} \quad (40)$$

We next show that the optimal power allocation dictates that the energy is saved till the last slot and transmitted then, i.e.,

$$P_i^* = 0, \quad i \leq D-1, \quad \text{and} \quad P_D^* = \sum_{i=1}^D E_i \quad (41)$$

This can be proved by developing an upper bound as follows:

$$\sum_{i=1}^D \frac{P_i}{\sum_{k=1}^{i-1} \alpha^{i-1-k} P_k + \Gamma_0} \leq \sum_{i=1}^D \frac{P_i}{\Gamma_0} \quad (42)$$

$$\leq \frac{\sum_{i=1}^D E_i}{\Gamma_0} \quad (43)$$

and noting that this bound is achieved by the claimed power allocation.

A sufficient condition to have a low SINR regime is $\sum_{i=1}^D E_i \ll \Gamma_0$. The temperature at the end of the communication session is equal to $T_{max} = \beta \sum_{i=1}^D E_i + T_e$. Also, the optimal power allocation does not need the non-causal knowledge of the energy arrival process, as all the harvested energy is used in the last slot.

B. High SINR Case

When the values of c and σ are small, SINR is high and we approximate the objective function by ignoring 1 inside the logarithm, i.e., $\log(1+x) \approx \log(x)$. Hence, the problem in (34) can be written as:

$$\begin{aligned} & \max_{\mathbf{P} \geq \mathbf{0}} \sum_{i=1}^D \frac{1}{2} \log \left(\frac{P_i}{\sum_{k=1}^{i-1} \alpha^{i-1-k} P_k + \Gamma_0} \right) \\ & \text{s.t. } \sum_{i=1}^k P_i \leq \sum_{i=1}^k E_i, \quad \forall k \end{aligned} \quad (44)$$

The problem in (44) has the Lagrangian:

$$\begin{aligned} \mathcal{L} = & - \sum_{i=1}^D \log \left(\frac{P_i}{\sum_{k=1}^{i-1} \alpha^{i-1-k} P_k + \Gamma_0} \right) \\ & + \sum_{k=1}^D \mu_k \left(\sum_{i=1}^k P_i - \sum_{i=1}^k E_i \right) \end{aligned} \quad (45)$$

Taking the derivative with respect to P_i gives,

$$\frac{\partial \mathcal{L}}{\partial P_i} = -\frac{1}{P_i} + \sum_{j=i+1}^D \frac{\alpha^{j-1-i}}{\sum_{k=1}^{j-1} \alpha^{j-1-k} P_k + \Gamma_0} + \sum_{k=i}^D \mu_k \quad (46)$$

and then equating to zero gives:

$$\frac{1}{P_i} - \sum_{j=i+1}^D \frac{\alpha^{j-1-i}}{\sum_{k=1}^{j-1} \alpha^{j-1-k} P_k + \Gamma_0} = \sum_{k=i}^D \mu_k \quad (47)$$

Although the problem in (44) is non-convex, it is a geometric program and we show next that any local optimal solution for this problem is globally optimal. To show this, we consider the following equivalent problem:

$$\begin{aligned} & \min_{\mathbf{x} \in \mathbb{R}^D} \sum_{i=1}^D \frac{1}{2} \log \left(\frac{\sum_{k=1}^{i-1} \alpha^{i-1-k} e^{x_k} + \Gamma_0}{e^{x_i}} \right) \\ & \text{s.t. } \sum_{i=1}^k e^{x_i} \leq \sum_{i=1}^k E_i, \quad \forall k \end{aligned} \quad (48)$$

This equivalent problem is obtained by substituting $P_i = e^{x_i}$ and letting $x_i \in \mathbb{R}$. The equivalent problem in (48) is a convex optimization problem since the objective is a convex function

in the form of a log-sum-exponent and the constraint set is a convex set [46]. Hence, the KKTs are necessary and sufficient for global optimality. We show this as follows.

We first write the Lagrangian of problem (48) as:

$$\mathcal{L} = -\sum_{i=1}^D \log \left(\frac{e^{x_i}}{\sum_{k=1}^{i-1} \alpha^{i-1-k} e^{x_k} + \Gamma_0} \right) + \sum_{k=1}^D \nu_k \left(\sum_{i=1}^k e^{x_i} - \sum_{i=1}^k E_i \right) \quad (49)$$

Taking the derivative with respect to x_i gives,

$$\frac{\partial \mathcal{L}}{\partial x_i} = -1 + \sum_{j=i+1}^D \frac{\alpha^{j-1-i} e^{x_i}}{\sum_{k=1}^{j-1} \alpha^{j-1-k} e^{x_k} + \Gamma_0} + e^{x_i} \sum_{k=i}^D \nu_k \quad (50)$$

which provides the following necessary condition:

$$e^{-x_i} - \sum_{j=i+1}^D \frac{\alpha^{j-1-i}}{\sum_{k=1}^{j-1} \alpha^{j-1-k} e^{x_k} + \Gamma_0} = \sum_{k=i}^D \nu_k \quad (51)$$

Using the transformation $x_i = \log(P_i)$ and setting $\nu_i = \mu_i$, we observe that any solution of (47) satisfies (51). Also, complementary slackness corresponding to (45) is satisfied if and only if it is satisfied by those for (49). Since the equivalent problem in (48) is convex, any solution satisfying the KKTs is global optimal and through the transformation $x_i = \log(P_i)$, $\mu_i = \nu_i$ is also global optimal in the original problem in (44).

The equivalent problem in (48) can be solved using any convex optimization toolbox. We further note that the equivalent problem and the original problem both have unique solutions. More generally, for any fixed multipliers μ , the primal problem of minimizing the Lagrangian function in (45) has a unique solution. This follows because the Lagrangian function in (49) is strictly convex as it is formed with strictly convex constraint functions and a convex objective function; for fixed Lagrange multipliers the Lagrangian function in (49) is strictly convex.

We now focus on the KKT conditions of the original problem (44). Our ultimate goal in the following discussion is to show that the optimal solution of (44) has a power allocation which is monotone increasing in time index i , that is, $P_i \leq P_{i+1}$. We prove this by showing that the solution of the corresponding KKTs in (47) with an arbitrary $\mu \geq 0$ is monotone increasing in time index i , hence, this also follows for the optimal μ^* . We provide the proof for this fact in Appendix A. The proof is enabled by developing an algorithm with an update rule which satisfies the properties of *standard interference functions* introduced in [47]. Hence, from [47, Th. 2], the algorithm converges to a unique fixed point. We then show that the power allocation at this unique fixed point is monotone increasing in time. Then, from strict convexity of this problem, we know that KKTs in (47) have a unique solution. Hence, our algorithm converges to the unique solution of the KKTs in (47) and this solution has monotone increasing power allocations. When compared to its predecessors in [9]–[14], our method yields a more general class of problems in which optimal power allocation is monotone increasing under energy harvesting constraints. We also note

that due to [7, Lemma 3] and since the powers are monotone increasing, the temperature sequence T_i^* resulting from the optimal power allocation P_i^* is also monotone increasing.

In order to obtain the optimal solution, one has to determine the optimal Lagrange multipliers μ^* and the power allocation \mathbf{P} . This can be done numerically by using standard techniques for constrained convex optimization. In particular, one can use projected gradient descent [46] in the equivalent convex problem in (48) to determine μ^* and corresponding power allocation.

V. EXPLICIT AND IMPLICIT TEMPERATURE CONSTRAINTS

In this section, we consider the case when both implicit and explicit temperature constraints are active. In this case, the temperature controls the channel quality and is also constrained by a critical level. This problem is in the following form:

$$\begin{aligned} \max_{\mathbf{P} \geq 0} \quad & \sum_{i=1}^D \frac{1}{2} \log \left(1 + \frac{P_i}{\sum_{k=1}^{i-1} \alpha^{i-1-k} P_k + \Gamma_0} \right) \\ \text{s.t.} \quad & \sum_{i=1}^k \alpha^{k-i} P_i \leq \frac{T_c - T_e}{\beta} \\ & \sum_{i=1}^k P_i \leq \sum_{i=1}^k E_i, \quad \forall k \end{aligned} \quad (52)$$

which is a non-convex optimization problem. We can tackle the challenge due to non-convexity here as we did in Section IV. In particular, in the general SINR case, one can reach a local optimal solution for problem (52) using the signomial programming approach described there. On the other hand, in the low SINR case, the objective function in (52) is approximated by $\sum_{i=1}^D \frac{P_i}{\sum_{k=1}^{i-1} \alpha^{i-1-k} P_k + \Gamma_0}$ and it is a fractional program which can in general be mapped to a linear program.

The problem in (52) possesses some of the properties of the problem with explicit temperature constraints only studied in Section III. In particular, if the temperature constraint is tight for two consecutive slots in the optimal solution, then the power level in the second slot must be equal to $\frac{T_c - T_e}{\beta}(1 - \alpha)$. Additionally, when the temperature at the end of a slot hits T_c for the first time, then the power in that slot must be strictly higher than $\frac{T_c - T_e}{\beta}(1 - \alpha)$. We also note that the problem reduces to the case of implicit temperature constraint when the energy arrivals satisfy $\sum_{i=1}^D E_i \leq \frac{T_c - T_e}{\beta}$ as the explicit temperature constraint is never tight in this case.

In the high SINR case, we have $\log(1+x) \approx \log(x)$ and the problem (52) is a geometric program which can be transformed to an equivalent convex problem. In general, the optimal power sequence does not have a monotonic structure in this case. When harvested energies are sufficiently large and the energy constraints are not binding, and if $\alpha \leq \frac{\beta \Gamma_0}{T_c - T_e + \beta \Gamma_0}$, then the optimal power sequence P_i is monotone decreasing and when the temperature hits T_c , the power becomes constant and is equal to $\frac{(T_c - T_e)(1 - \alpha)}{\beta}$. Furthermore, under this condition the temperature is monotone increasing. We provide the proof for these facts in Appendix B.

VI. NUMERICAL RESULTS

In this section we illustrate our analytical findings in the earlier parts of this paper. We consider a wireless communication setting inspired by biomedical implant communications with reasonably high bandwidth. We consider a band-limited additive Gaussian noise channel with communication bandwidth of $B = 5$ MHz and a noise spectral density of $N_0 = 2 \times 10^{-19}$ W/Hz. Moreover, we let the pathloss coefficient between the transmitter and the receiver be denoted by h and we set this coefficient as 60 dB for all the scenarios we consider below. We assume that this coefficient remains constant throughout the communication duration. We set the slot length to $\Delta = 1$ second. With these system parameters in place, the total throughput over the $[0, D]$ interval is expressed in the explicit temperature constrained scenario as follows:

$$T_S = \sum_{i=1}^D \frac{\Delta}{2} \log_2 \left(1 + \frac{hP_i}{N_0 B} \right) \quad (53)$$

$$= \sum_{i=1}^D \frac{1}{2} \log_2 \left(1 + \frac{P_i}{10^{-6}} \right) \text{ Bits/Hz} \quad (54)$$

The total throughput, in Bits/Hz, for the implicit temperature constrained scenario is:

$$T_S = \sum_{i=1}^D \frac{\Delta}{2} \log_2 \left(1 + \frac{hP_i}{c \left(\beta \sum_{k=1}^{i-1} \alpha^{i-1-k} hP_k + T_e \right) + N_0 B} \right) \quad (55)$$

$$= \sum_{i=1}^D \frac{1}{2} \log_2 \left(1 + \frac{P_i}{c \beta \sum_{k=1}^{i-1} \alpha^{i-1-k} P_k + c T_e 10^6 + 10^{-6}} \right) \quad (56)$$

In particular, the noise power term $c \left(\beta \sum_{k=1}^{i-1} \alpha^{i-1-k} hP_k + T_e \right)$ corresponds to the thermal noise at the receiver circuitry. In the ensuing numerical results, we will let the initial temperature be $T_e = 37$ °C throughout.

A. Explicit Temperature Constraints Only

In this subsection, we consider explicit peak temperature constraints only. We set the parameters to $a = 0.9 \frac{\text{°C}}{\text{W.sec}}$ and $b = 1 \text{ sec}^{-1}$. We consider an energy arrival profile $E = [100, 200, 20, 70, 200]$ mJ. Initially, we consider a critical temperature level of $T_c = 37.1$ °C. We observe the resulting power profile in Fig. 2. Next, we illustrate the variations of the optimal total throughput with respect to a and b parameters in Figs. 3(a) and 3(b). As the value of a increases, the explicit temperature constraint becomes the limiting constraint and we observe that the total throughput decreases as in Figs. 3(a). In contrast, we observe that as the value of b increases, the explicit temperature constraint becomes less binding and the total throughput increases as in Fig. 3(b).

Next, we consider the temperature limited case under explicit temperature constraints. For this case, we set $T_c = 37.2$ °C. We observe in Fig. 4 that in the temperature limited regime the power is strictly decreasing and the temperature is strictly increasing until it reaches the critical level.

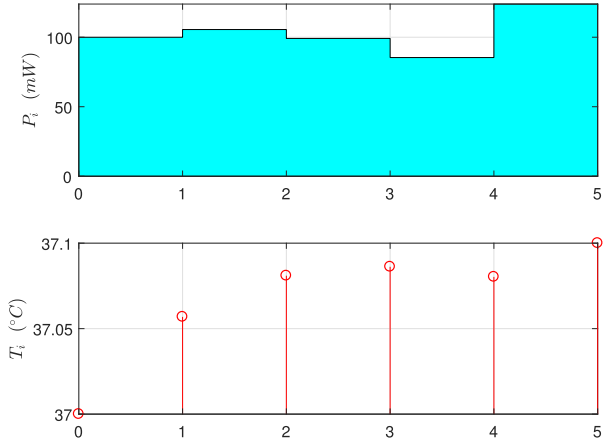
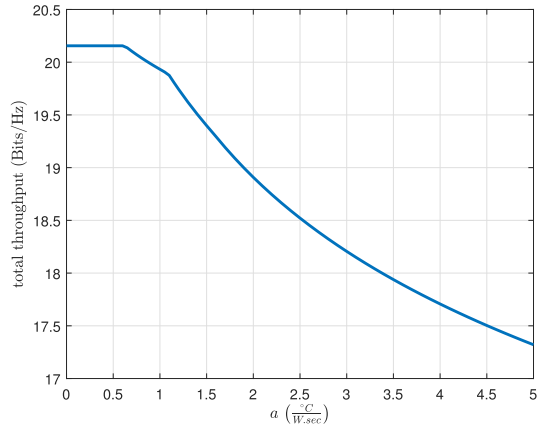
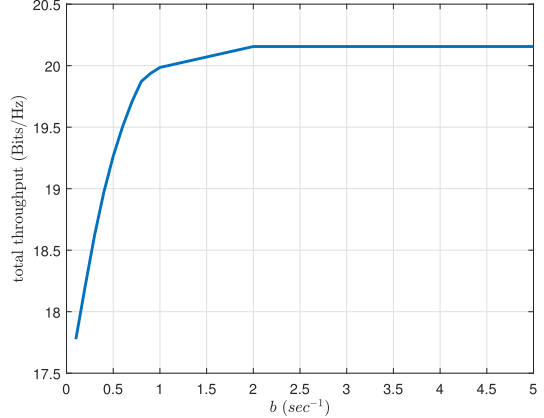


Fig. 2. Illustration of optimal power policy and resulting temperature profile in the general case for explicit temperature constraints.



(a) Variation with respect to the parameter a .



(b) Variation with respect to the parameter b .

Fig. 3. Variation of the optimal total throughput with respect to the temperature related parameters a and b under a critical temperature constraint $T_c = 38$ °C.

B. Implicit Temperature Constraints Only

In this subsection, we consider the scenario with implicit temperature constraints only and the energy arrival profile $E = [100, 30, 50, 70]$ mJ. We set the parameters $a = 0.9 \frac{\text{°C}}{\text{W.sec}}$ and $b = 1 \text{ sec}^{-1}$. In Fig. 5(a) and Fig. 5(b), we observe

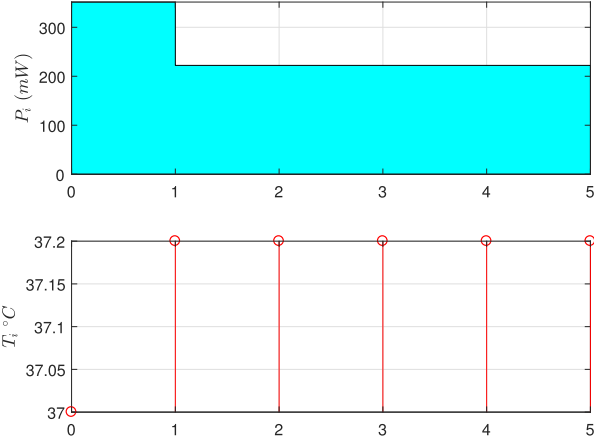
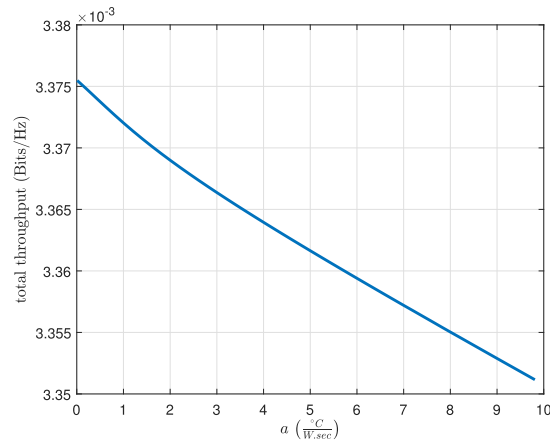
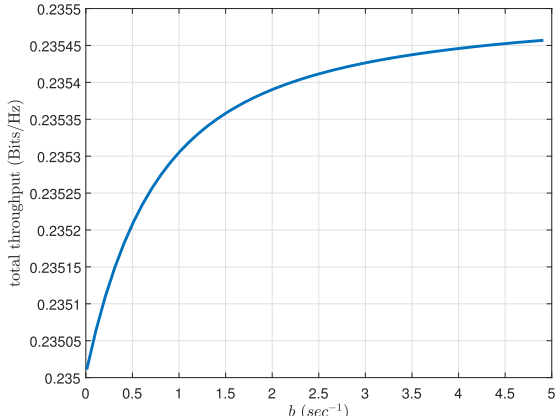


Fig. 4. Illustration of optimal power policy and resulting temperature profile in the temperature limited regime for explicit temperature constraints.



(a) Variation with respect to the parameter a .



(b) Variation with respect to the parameter b .

Fig. 5. Variation of the optimal rate with respect to the temperature related parameters a and b in an implicitly temperature constrained scenario.

the monotonic variations of the optimal total throughput with respect to the parameters a and b , respectively. For Fig. 5(a), we use $c = 10^{-6} \frac{W}{^{\circ}C}$ while for Fig. 5(b), we use $c = 1.35 \times 10^{-8} \frac{W}{^{\circ}C}$.

Next, we consider the high SINR regime for the same scenario with the energy arrival profile $E = [30, 70, 20, 80]$ mJ.

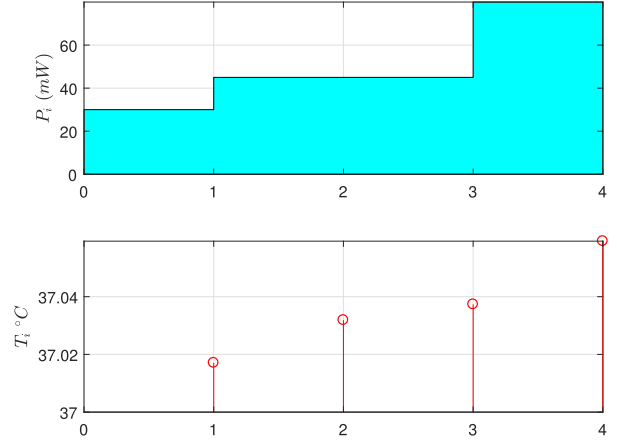


Fig. 6. Illustration of optimal power policy and resulting temperature profile in the high SINR regime for implicit temperature constraints.

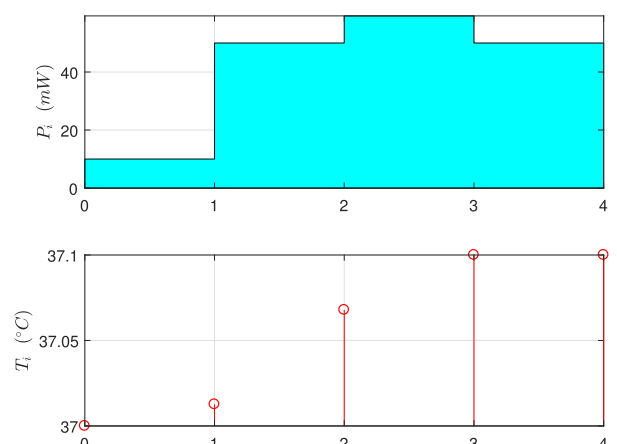


Fig. 7. Illustration of optimal power policy and resulting temperature profile in the high SINR regime for simultaneous implicit and explicit temperature constraint.

The parameter determining the thermal noise is taken as $c = 10^{-12} \frac{W}{^{\circ}C}$ so that the SINR is guaranteed to be significantly larger than 1. In Fig. 6, we observe that the optimal power allocation is monotone increasing as we proved in our analytical results.

C. Simultaneous Explicit and Implicit Temperature Constraints

In the last subsection of numerical results, we consider the case when implicit and explicit temperature constraints are simultaneously active. In particular, we focus on the high SINR regime. We consider an energy arrival profile of $E = [10, 50, 200, 10]$ mJ. We set the two parameters as $a = 2 \frac{^{\circ}C}{W.sec}$, $b = 1 \text{ sec}^{-1}$ and the critical temperature to $T_c = 37.1 \text{ }^{\circ}C$. For this case, we set $c = 10^{-12} \frac{W}{^{\circ}C}$ so that the high SINR asymptotic is achieved. We observe the optimal power and resulting temperature profiles in Fig. 7.

We finally consider the high SINR case when the system is temperature limited. For this case, we update the parameter b as $b = 0.5 \text{ sec}^{-1}$ and the critical temperature as $T_c = 38 \text{ }^{\circ}C$. We show the optimal power allocation and the

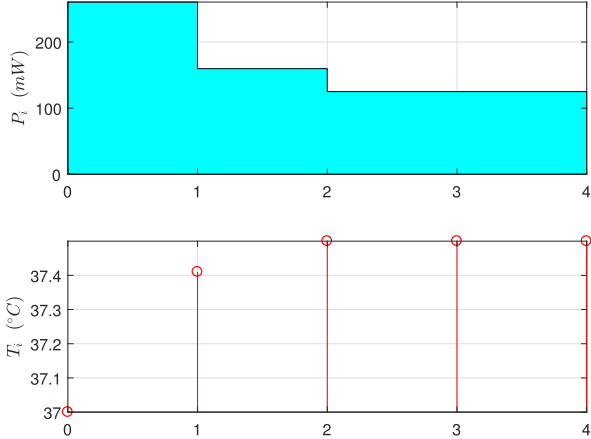


Fig. 8. Illustration of optimal power policy and resulting temperature profile in the temperature limited high SINR regime for simultaneous implicit and explicit temperature constraint.

resulting temperature profile in Fig. 8. Note that optimal power sequence is monotone decreasing, corresponding temperature sequence is monotone increasing and the power level remains constant when the temperature hits the critical level.

VII. CONCLUSION

We considered explicit and implicit temperature constraints in a single-user energy harvesting communication system in discrete time. Under explicit temperature constraints, the temperature is imposed to be less than a critical level. In this case, we studied optimal power allocation for multiple energy arrivals. For the temperature limited regime, we showed that the optimal power sequence is monotone decreasing while the temperature of the system is monotone increasing. Next, we considered an implicit temperature constraint where the temperature level affects channel quality. We studied the general case as well as the high and low SINR cases. In the low SINR case, we showed that the optimal allocation dictates the transmitter to save its harvested energy till the last slot and transmit all the harvested energy then. In the high SINR case, we observed that the problem is a geometric program and we expanded upon its equivalent convex version to show that optimal power allocation is monotone increasing in time. Finally, we considered the case in which implicit and explicit temperature constraints are simultaneously active. We identified a sufficient condition on the system parameters that results in a monotone decreasing optimal power allocation. Our current investigation leaves several directions to pursue in future research, such as, optimal power allocation for the finite battery case; online power allocation under explicit and implicit temperature constraints; explicit and implicit temperature constraints in multi-user settings such as broadcast and multiple access channels.

APPENDIX A

PROOF OF THE MONOTONICITY OF OPTIMAL POWER ALLOCATION OF PROBLEM (44)

In this appendix, we present the proof for the monotonicity of the optimal power allocation for the problem in (44).

We rewrite its KKTs in (47) as follows:

$$\frac{1}{P_i} = \sum_{k=i}^D \mu_k + \sum_{j=i+1}^D \frac{\alpha^{j-1-i}}{\sum_{k=1}^{j-1} \alpha^{j-1-k} P_k + \Gamma_0} \quad (57)$$

Based on this equation, for a fixed μ , we now define an update rule to solve for the power allocation P_i iteratively as follows:

$$P_i(\mathbf{P}) \triangleq \frac{1}{\sum_{k=i}^D \mu_k + \sum_{j=i+1}^D \frac{\alpha^{j-1-i}}{\sum_{k=1}^{j-1} \alpha^{j-1-k} P_k + \Gamma_0}} \quad (58)$$

where the function $P_i(\mathbf{P})$ calculates the updated power P_i when the powers are equal to \mathbf{P} . The algorithm proceeds as follows: We first initialize the power allocation with any arbitrary non-negative power allocation \mathbf{P}^0 , where the superscript denotes the iteration index. We then substitute with \mathbf{P}^0 in (58) to obtain the new power allocation \mathbf{P}^1 , where $\mathbf{P}^1 \triangleq (P_1(\mathbf{P}^0), \dots, P_D(\mathbf{P}^0))$. Similarly, we use the powers \mathbf{P}^1 to obtain the updated powers \mathbf{P}^2 , and repeat this process. We show next that this algorithm converges to a unique fixed point.

To show that these updates converge to a unique fixed point, we first present the following definition of a *standard interference function* [47]:

Definition 1: Interference function $I(\mathbf{P})$ is standard if for all $\mathbf{P} \geq 0$ the following properties are satisfied:

- *Positivity*: $I(\mathbf{P}) > 0$.
- *Monotonicity*: If $\mathbf{P} \geq \mathbf{P}'$, then $I(\mathbf{P}) \geq I(\mathbf{P}')$.
- *Scalability*: For all $\theta > 1$, $\theta I(\mathbf{P}) \geq I(\theta \mathbf{P})$.

Now, we want to show that the update rule $I(\mathbf{P}) = (P_1(\mathbf{P}), P_2(\mathbf{P}), \dots, P_D(\mathbf{P}))$ is a standard function, i.e., it satisfies the three properties above.

The positivity property follows from,

$$P_i(\mathbf{P}) \geq \frac{1}{\sum_{j=i}^D \mu_j} \geq \frac{1}{\mu_D} > 0 \quad (59)$$

where $\mu_D > 0$ follows from (47) with $i = D$ and since the power P_D is finite due to the finite energy constraint.

The monotonicity property follows since the denominator of $P_i(\mathbf{P})$ is a decreasing function of the powers, and hence, $P_i(\mathbf{P})$ is an increasing function of the powers.

The scalability property follows from the following for $\theta > 1$,

$$P_i(\theta \mathbf{P}) = \frac{1}{\sum_{k=i}^D \mu_k + \sum_{j=i+1}^D \frac{\alpha^{j-1-i}}{\sum_{k=1}^{j-1} \alpha^{j-1-k} \theta P_k + \Gamma_0}} \quad (60)$$

$$= \frac{\theta}{\theta \sum_{k=i}^D \mu_k + \sum_{j=i+1}^D \frac{\alpha^{j-1-i}}{\sum_{k=1}^{j-1} \alpha^{j-1-k} P_k + \frac{\Gamma_0}{\theta}}} \quad (61)$$

$$< \frac{\theta}{\sum_{k=i}^D \mu_k + \sum_{j=i+1}^D \frac{\alpha^{j-1-i}}{\sum_{k=1}^{j-1} \alpha^{j-1-k} P_k + \Gamma_0}} \quad (62)$$

$$= \theta P_i(\mathbf{P}) \quad (63)$$

This completes the proof that $I(\mathbf{P}) = (P_1(\mathbf{P}), P_2(\mathbf{P}), \dots, P_D(\mathbf{P}))$ in (58) is a standard interference function.

From [47, Th. 2], we now conclude that the algorithm in (58) converges to a *unique* fixed point. From the equivalence of (44) to the strictly convex problem in (48), we know that there is only one unique solution to the equations in (47), and

hence, the algorithm in (58) converges to the unique power allocation which solves the KKTs in (47).

It now remains to show that at this unique fixed point, the power allocation is monotone increasing in time. We prove this by showing that if we begin with any arbitrary monotone increasing power allocation, the update algorithm retains this ordering for the power allocation in each iteration, and hence, in the limit. To show this, let us assume that we have an arbitrary power vector \mathbf{P} which satisfies $P_i \leq P_{i+1}$ for all $i = \{1, \dots, D-1\}$. We want to show that $P_i(\mathbf{P}) \leq P_{i+1}(\mathbf{P})$. This follows from:

$$P_{i+1}(\mathbf{P}) = \frac{1}{\sum_{k=i+1}^D \mu_k + \sum_{j=i+2}^D \frac{\alpha^{j-2-i}}{\sum_{k=1}^{j-1} \alpha^{j-1-k} P_k + \Gamma_0}} \quad (64)$$

$$\geq \frac{1}{\sum_{k=i}^D \mu_k + \sum_{j=i+2}^D \frac{\alpha^{j-2-i}}{\sum_{k=1}^{j-1} \alpha^{j-1-k} P_k + \Gamma_0}} \quad (65)$$

$$\geq \frac{1}{\sum_{k=i}^D \mu_k + \sum_{j=i+2}^D \frac{\alpha^{j-2-i}}{\sum_{k=2}^{j-1} \alpha^{j-1-k} P_k + \Gamma_0}} \quad (66)$$

$$= \frac{1}{\sum_{k=i}^D \mu_k + \sum_{j=i+2}^D \frac{\alpha^{j-2-i}}{\sum_{k=1}^{j-2} \alpha^{j-2-k} P_{k+1} + \Gamma_0}} \quad (67)$$

$$\geq \frac{1}{\sum_{k=i}^D \mu_k + \sum_{j=i+2}^D \frac{\alpha^{j-2-i}}{\sum_{k=1}^{j-2} \alpha^{j-2-k} P_k + \Gamma_0}} \quad (68)$$

$$\geq \frac{1}{\sum_{k=i}^D \mu_k + \sum_{j=i+1}^{D-1} \frac{\alpha^{j-1-i}}{\sum_{k=1}^{j-1} \alpha^{j-1-k} P_k + \Gamma_0}} \quad (69)$$

$$\geq \frac{1}{\sum_{k=i}^D \mu_k + \sum_{j=i+1}^{D-1} \frac{\alpha^{j-1-i}}{\sum_{k=1}^{j-1} \alpha^{j-1-k} P_k + \Gamma_0}} \quad (70)$$

$$= P_i(\mathbf{P}) \quad (71)$$

where (65) follows by adding the non-negative Lagrange multiplier μ_i in the denominator, (66) follows by neglecting positive terms in the denominator in the second term of the denominator, (67) follows by replacing $\sum_{k=2}^{j-1}$ by $\sum_{k=1}^{j-2}$ and changing the indices inside the summation accordingly, (68) follows since we have $P_k \leq P_{k+1}$, (69) follows by replacing $\sum_{j=i+2}^D$ by $\sum_{j=i+1}^{D-1}$ and changing the indices inside the summation accordingly, and (70) follows by adding a positive term in the denominator. Since in each iteration the power is monotone increasing, the power allocation will also be monotone increasing at the fixed point.

APPENDIX B

PROOF OF THE MONOTONICITY OF THE OPTIMAL POWER ALLOCATION OF PROBLEM (52) WHEN $\alpha \leq \frac{\beta\Gamma_0}{T_c - T_e + \beta\Gamma_0}$

We start the proof by noting that the KKT conditions and the complementary slackness conditions for the problem in (52) are necessary and sufficient for optimality.

Let us now define i_1^* as the first slot at which the temperature hits T_c . Since $\mu_k = 0$ for $k = 1, \dots, i_1^* - 1$, KKT conditions in the integer interval $[1 : i_1^*]$ are in the following form:

$$\frac{1}{P_i} - \sum_{j=i+1}^D \frac{1}{\sum_{k=1}^{j-1} \alpha^{i-k} P_k + \Gamma_{j-1-i}} = \alpha^{-i} W, \quad i = 1, \dots, i_1^* \quad (72)$$

where $W \triangleq \sum_{k=i_1^*}^D \alpha^k \mu_k$. By comparing (72) for i and $i+1 \leq i_1^*$, we have:

$$\frac{1}{P_i} - \frac{1}{\sum_{k=1}^i \alpha^{i-k} P_k + \Gamma_0} = \frac{\alpha}{P_{i+1}} \quad (73)$$

We now rewrite (73) as follows:

$$P_{i+1} = \alpha \frac{\sum_{k=1}^{i-1} \alpha^{i-k} P_k + P_i + \Gamma_0}{\sum_{k=1}^{i-1} \alpha^{i-k} P_k + \Gamma_0} P_i \quad (74)$$

$$= \alpha \left(1 + \frac{P_i}{\sum_{k=1}^{i-1} \alpha^{i-k} P_k + \Gamma_0} \right) P_i \quad (75)$$

Now, due to the temperature constraints, we have $P_i \leq \frac{T_c - T_e}{\beta}$ for all i and $\frac{P_i}{\sum_{k=1}^{i-1} \alpha^{i-k} P_k + \Gamma_0} \leq \frac{T_c - T_e}{\beta \Gamma_0}$. Hence, under the assumed condition on α , we have

$$\alpha \left(1 + \frac{P_i}{\sum_{k=1}^{i-1} \alpha^{i-k} P_k + \Gamma_0} \right) \leq 1 \quad (76)$$

This proves that $P_{i+1} \leq P_i$ for all $i \in [1 : i_1^* - 1]$, i.e., the optimal power allocation is non-increasing in the slots $\{1, \dots, i_1^*\}$.

Now, if the temperature drops below T_c after slot i_1^* , say at slot i_2^* , the KKT conditions will have the form identical to (72) in the interval $[i_1^* + 1 : i_2^*]$. Following the steps, we have that $P_{i+1} \leq P_i$ for $[i_1^* + 1 : i_2^*]$, i.e., the optimal power allocation is non-increasing in the slots $\{i_1^* + 1, \dots, i_2^*\}$. It remains to show that the power allocation is also non-increasing between slots i_1^* and $i_1^* + 1$. Note that it follows that the power in slot i_1^* is strictly higher than $\frac{(T_c - T_e)(1-\alpha)}{\beta}$, while in slot $i_1^* + 1$ the power can be no larger than $\frac{(T_c - T_e)(1-\alpha)}{\beta}$ as otherwise this violates the temperature constraint. Hence, the power allocation between slots i_1^* and $i_1^* + 1$ is non-increasing also. This concludes the proof of the first part. The proof of the monotonicity of the resulting temperature follows similar to (21)-(28).

REFERENCES

- [1] H. Ren and M. Q.-H. Meng, "Rate control to reduce bioeffects in wireless biomedical sensor networks," in *Proc. IEEE Annu. Int. Conf. Mobile Ubiquitous Syst.*, Jul. 2006, pp. 1-7.
- [2] S. Ullah *et al.*, "A comprehensive survey of wireless body area networks," *J. Med. Syst.*, vol. 36, no. 3, pp. 1065-1094, Jun. 2012.
- [3] B. Latré, B. Braem, I. Moerman, C. Blondia, and P. Demeester, "A survey on wireless body area networks," *J. Wireless Netw.*, vol. 17, no. 1, pp. 1-18, 2011.
- [4] Q. Tang, N. Tummala, S. K. S. Gupta, and L. Schwiebert, "Communication scheduling to minimize thermal effects of implanted biosensor networks in homogeneous tissue," *IEEE Trans. Biomed. Eng.*, vol. 52, no. 7, pp. 1285-1294, Jul. 2005.
- [5] A. Mutapcic, S. Boyd, S. Murali, D. Atienza, G. D. Micheli, and R. Gupta, "Processor speed control with thermal constraints," *IEEE Trans. Circuits Syst. I, Reg. Papers*, vol. 56, no. 9, pp. 1994-2008, Sep. 2009.
- [6] D. Forte and A. Srivastava, "Thermal-aware sensor scheduling for distributed estimation," *ACM Trans. Sensor Netw.*, vol. 9, no. 4, pp. 53:1-53:31, Jul. 2013.
- [7] O. Ozel, S. Ulukus, and P. Grover, "Energy harvesting transmitters that heat up: Throughput maximization under temperature constraints," *IEEE Wireless Commun.*, vol. 15, no. 8, pp. 5440-5452, Aug. 2016.
- [8] A. Baknina, O. Ozel, and S. Ulukus, "Energy harvesting communications under temperature constraints," in *Proc. ITA*, Jan./Feb. 2016, pp. 1-10.

[9] J. Yang and S. Ulukus, "Optimal packet scheduling in an energy harvesting communication system," *IEEE Trans. Commun.*, vol. 60, no. 1, pp. 220–230, Jan. 2012.

[10] K. Tutuncuoglu and A. Yener, "Optimum transmission policies for battery limited energy harvesting nodes," *IEEE Trans. Wireless Commun.*, vol. 11, no. 3, pp. 1180–1189, Mar. 2012.

[11] O. Ozcel, K. Tutuncuoglu, J. Yang, S. Ulukus, and A. Yener, "Transmission with energy harvesting nodes in fading wireless channels: Optimal policies," *IEEE J. Sel. Areas Commun.*, vol. 29, no. 8, pp. 1732–1743, Sep. 2011.

[12] C. K. Ho and R. Zhang, "Optimal energy allocation for wireless communications with energy harvesting constraints," *IEEE Trans. Signal Process.*, vol. 60, no. 9, pp. 4808–4818, Sep. 2012.

[13] J. Yang, O. Ozcel, and S. Ulukus, "Broadcasting with an energy harvesting rechargeable transmitter," *IEEE Trans. Wireless Commun.*, vol. 11, no. 2, pp. 571–583, Feb. 2012.

[14] J. Yang and S. Ulukus, "Optimal packet scheduling in a multiple access channel with energy harvesting transmitters," *J. Commun. Netw.*, vol. 14, no. 2, pp. 140–150, Apr. 2012.

[15] Z. Wang, V. Aggarwal, and X. Wang, "Iterative dynamic water-filling for fading multiple-access channels with energy harvesting," *IEEE J. Sel. Areas Commun.*, vol. 33, no. 3, pp. 382–395, Mar. 2015.

[16] K. Tutuncuoglu and A. Yener, "Sum-rate optimal power policies for energy harvesting transmitters in an interference channel," *J. Commun. Netw.*, vol. 14, no. 2, pp. 151–161, Apr. 2012.

[17] O. Orhan and E. Erkip, "Energy harvesting two-hop communication networks," *IEEE J. Sel. Areas Commun.*, vol. 33, no. 12, pp. 2658–2670, Dec. 2015.

[18] D. Gündüz and B. Devillers, "Two-hop communication with energy harvesting," in *Proc. IEEE CAMSAP*, Dec. 2011, pp. 201–204.

[19] C. Huang, R. Zhang, and S. Cui, "Throughput maximization for the Gaussian relay channel with energy harvesting constraints," *IEEE J. Sel. Areas Commun.*, vol. 31, no. 8, pp. 1469–1479, Aug. 2013.

[20] B. Varan and A. Yener, "Delay constrained energy harvesting networks with limited energy and data storage," *IEEE J. Sel. Areas Commun.*, vol. 34, no. 5, pp. 1550–1564, May 2016.

[21] A. Arafa, A. Baknina, and S. Ulukus, "Energy harvesting two-way channels with decoding and processing costs," *IEEE Trans. Green Commun. Netw.*, vol. 1, no. 1, pp. 3–16, Mar. 2017.

[22] B. Gurakan and S. Ulukus, "Cooperative diamond channel with energy harvesting nodes," *IEEE J. Sel. Areas Commun.*, vol. 34, no. 5, pp. 1604–1617, May 2016.

[23] B. Devillers and D. Gündüz, "A general framework for the optimization of energy harvesting communication systems with battery imperfections," *J. Commun. Netw.*, vol. 14, no. 2, pp. 130–139, Apr. 2012.

[24] O. Orhan, D. Gündüz, and E. Erkip, "Energy harvesting broadband communication systems with processing energy cost," *IEEE Trans. Wireless Commun.*, vol. 13, no. 11, pp. 6095–6107, Nov. 2014.

[25] J. Xu and R. Zhang, "Throughput optimal policies for energy harvesting wireless transmitters with non-ideal circuit power," *IEEE J. Sel. Areas Commun.*, vol. 32, no. 2, pp. 322–332, Feb. 2014.

[26] O. Ozcel, K. Shahzad, and S. Ulukus, "Optimal energy allocation for energy harvesting transmitters with hybrid energy storage and processing cost," *IEEE Trans. Signal Process.*, vol. 62, no. 12, pp. 3232–3245, Jun. 2014.

[27] K. Tutuncuoglu, A. Yener, and S. Ulukus, "Optimum policies for an energy harvesting transmitter under energy storage losses," *IEEE J. Sel. Areas Commun.*, vol. 33, no. 3, pp. 476–481, Mar. 2015.

[28] X. Wang, Z. Nan, and T. Chen, "Optimal MIMO broadcasting for energy harvesting transmitter with non-ideal circuit power consumption," *IEEE Trans. Wireless Commun.*, vol. 14, no. 5, pp. 2500–2512, May 2015.

[29] X. Chen, W. Ni, X. Wang, and Y. Sun, "Optimal quality-of-service scheduling for energy-harvesting powered wireless communications," *IEEE Trans. Wireless Commun.*, vol. 15, no. 5, pp. 3269–3280, May 2016.

[30] K. Tutuncuoglu and A. Yener, "Communicating with energy harvesting transmitters and receivers," in *Proc. ITA*, Feb. 2012, pp. 240–245.

[31] H. Mahdavi-Doost and R. D. Yates, "Energy harvesting receivers: Finite battery capacity," in *Proc. IEEE ISIT*, Jul. 2013, pp. 1799–1803.

[32] R. D. Yates and H. Mahdavi-Doost, "Energy harvesting receivers: Optimal sampling and decoding policies," in *Proc. IEEE GlobalSIP*, Dec. 2013, pp. 367–370.

[33] H. Mahdavi-Doost and R. D. Yates, "Fading channels in energy-harvesting receivers," in *Proc. CISS*, Mar. 2014, pp. 1–6.

[34] J. Rubio, A. Pascual-Iserte, and M. Payaro, "Energy-efficient resource allocation techniques for battery management with energy harvesting nodes: A practical approach," in *Proc. Eur. Wireless Conf.*, Apr. 2013, pp. 1–6.

[35] A. Arafa and S. Ulukus, "Optimal policies for wireless networks with energy harvesting transmitters and receivers: Effects of decoding costs," *IEEE J. Sel. Areas Commun.*, vol. 33, no. 12, pp. 2611–2625, Dec. 2015.

[36] T. Koch, A. Lapidoth, and P. P. Sotiriadis, "Channels that heat up," *IEEE Trans. Inf. Theory*, vol. 55, no. 8, pp. 3594–3612, Aug. 2009.

[37] D. Ward, N. Martins, and B. M. Sadler, "Optimal remote estimation over action dependent switching channels: Managing workload and bias of a human operator," in *Proc. ACC*, Jul. 2015, pp. 3168–3174.

[38] T. Weissman, "Capacity of channels with action-dependent states," *IEEE Trans. Inf. Theory*, vol. 56, no. 11, pp. 5396–5411, Nov. 2010.

[39] B. Ahmadi and O. Simeone, "On channels with action-dependent states," in *Proc. IEEE ISIT*, Sep. 2012, pp. 167–171.

[40] M. Chiang, C. W. Tan, D. P. Palomar, D. O'neill, and D. Julian, "Power control by geometric programming," *IEEE Trans. Wireless Commun.*, vol. 6, no. 7, pp. 2640–2651, Jul. 2007.

[41] P. R. Gray and R. G. Meyer, *Analysis and Design of Analog Integrated Circuits*. Hoboken, NJ, USA: Wiley, 1990.

[42] B. R. Marks and G. P. Wright, "A general inner approximation algorithm for nonconvex mathematical programs," *Oper. Res.*, vol. 26, pp. 681–683, Jul. 1978.

[43] Y. Nesterov and A. Nemirovskii, *Interior-Point Polynomial Algorithms in Convex Programming*. Philadelphia, PA, USA: SIAM, 1994.

[44] M. Chiang, "Geometric programming for communication systems," *Found. Trends Commun. Inf. Theory*, vol. 2, nos. 1–2, pp. 1–154, 2005.

[45] S. Ulukus and L. J. Greenstein, "Throughput maximization in CDMA uplinks using adaptive spreading and power control," in *Proc. IEEE 6th ISSTA*, Sep. 2000, pp. 565–569.

[46] S. P. Boyd and L. Vandenberghe, *Convex Optimization*. Cambridge, U.K.: Cambridge Univ. Press, 2004.

[47] R. D. Yates, "A framework for uplink power control in cellular radio systems," *IEEE J. Sel. Areas Commun.*, vol. 13, no. 7, pp. 1341–1347, Sep. 1995.



Abdulrahman Baknina (S'09) received the B.Sc. degree in electrical engineering and the M.Sc. degree in wireless communications from Alexandria University, Alexandria, Egypt, in 2010 and 2013, respectively, and the Ph.D. degree in electrical and computer engineering, University of Maryland at College Park, College Park, MD, USA, in 2018. His research interests include optimization, information theory, and wireless communications.



Omur Ozcel (S'08–M'15) received the B.Sc. and M.S. degrees in electrical and electronics engineering from Middle East Technical University, Ankara, Turkey, and the Ph.D. degree in electrical and computer engineering from the University of Maryland at College Park, College Park. He was a Post-Doctoral Researcher with the Electrical Engineering and Computer Sciences Department, University of California at Berkeley, Berkeley. He is currently a Post-Doctoral Research Associate with the Electrical and Computer Engineering Department, Carnegie Mellon University. His research interests are in wireless communications, information theory, and networks.



Sennur Ulukus (S'90–M'98–SM'15–F'16) received the B.S. and M.S. degrees in electrical and electronics engineering from Bilkent University and the Ph.D. degree in electrical and computer engineering from the Wireless Information Network Laboratory, Rutgers University. She was a Senior Technical Staff Member at AT&T Labs-Research. She is a Professor of electrical and computer engineering with the University of Maryland (UMD) at College Park, where she also holds a joint appointment with the Institute for Systems Research (ISR). Her research interests are in wireless communications, information theory, signal processing, and networks, with recent focus on private information retrieval, timely status updates over networks, energy harvesting communications, information theoretic physical layer security, and wireless energy and information transfer.

Dr. Ulukus is a Distinguished Scholar-Teacher of the University of Maryland. She was a recipient of the 2003 IEEE Marconi Prize Paper Award in Wireless Communications, the 2005 NSF CAREER Award, the 2010–2011 ISR Outstanding Systems Engineering Faculty Award, and the 2012 ECE George Corcoran Education Award. She was a General TPC Co-Chair of 2017 IEEE ISIT, 2016 IEEE GLOBECOM, 2014 IEEE PIMRC, and 2011 IEEE CTW. She has been on the Editorial Board of the IEEE TRANSACTIONS ON GREEN COMMUNICATIONS AND NETWORKING since 2016. She was an Editor for the IEEE TRANSACTIONS ON COMMUNICATIONS (2003–2007), the IEEE TRANSACTIONS ON INFORMATION THEORY (2007–2010), and the IEEE JOURNAL ON SELECTED AREAS IN COMMUNICATIONS Series on Green Communications and Networking (2015–2016). She was a Guest Editor for the IEEE JOURNAL ON SELECTED AREAS IN COMMUNICATIONS (2015 and 2008), the IEEE TRANSACTIONS ON INFORMATION THEORY (2011), and the *Journal of Communications and Networks* (2012). She is a Distinguished Lecturer of the Information Theory Society 2018–2019.